15th Triennial World Congress, Barcelona, Spain

ADAPTIVE COMPENSATION OF TORQUE DISTURBANCES IN AN INDUSTRIAL ROBOT

Gianni Ferretti * **GianAntonio Magnani** * **Paolo Rocco** *

* *Dipartimento di Elettronica e Informazione, Politecnico di Milano, Piazza L. da Vinci 32, Milano, 20133, Italy, E-mail {ferretti,magnani,rocco}@elet.polimi.it*

Abstract: A compact model of torque disturbances in the brushless motors of an industrial manipulator is discussed and algorithms are given for the identification of model parameters. Thanks to its compactness, the model allows the implementation of a straightforward and effective technique for disturbance compensation. The compensation is adaptive as estimates of the parameters of the model are updated online. Experimental results are given to assess the effectiveness of the proposed approach.

Keywords: Brushless motors, Torque ripple, Industrial robots.

1. INTRODUCTION

The most common actuation system adopted in articulated robotic manipulators is by far a set of permanent magnets brushless motors connected to the links by transmission chains (or gearboxes). Brushless motors, however, introduce a disturbance in the system in the form of a ripple on the torque. This disturbance, associated to constructive imperfections in the motor and non ideal phase commutation, is pernicious, as it may excite the lightly damped dynamics of the mechanical structure.

A complete review of the methods used to minimize torque disturbances is reported in (Jahns and Soong, 1996). The techniques are classified into two main categories: motor-based, where the fundamental electromagnetic sources of the disturbance are addressed, and the design of the motor is adjusted in order to minimize them, and control-based, where active control schemes modify the excitation, to correct for any of the nonideal characteristics of the machine or its associated power inverter. Among this second class of techniques (the most pertinent with the present contribution) is the work by Jahns (Jahns, 1984), which proposes compensation of the disturbance effects through high bandwidth speed feedback. Selective elimination of torque ripple harmonics, through proper injection of harmonics of suitable orders in the current profiles, was first proposed in (Le-Huy *et al.*, 1986) and further extended in (Favre *et al.*, 1993), where an iterative procedure is worked out to eliminate higher order harmonics in the torque. In (Hanselman, 1994) and (Hung and Ding, 1993) the torque disturbance minimization is treated as a constrained optimization problem: the current profiles that minimize suitable functionals (related to the ohmic losses in the windings) and guarantee elimination of the torque harmonics up to a predetermined order, together with satisfaction of other constraints (such as Y connection of the phases), are computed, based on the known harmonics of the back EMF profiles. Inversion of the back EMF profiles of the single phases (computed by means of finite element analysis) is proposed in (Clenet *et al.*, 1993). Recently, Holtz and Springob (Holtz and Springob, 1996) have proposed a self-commissioning control scheme which identifies the machine parameters and adaptively controls the current using a standard microcontroller.

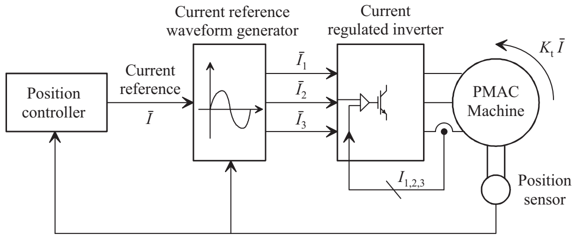

Fig. 1. Functional scheme of a brushless motor

In the present contribution, the problem is addressed starting from the formulation of a compact model of the torque pulsations in sinusoidal permanent magnet AC brushless motors (PMAC BLM) (Ferretti *et al.*, 1998*a*). The model defines the torque delivered by the motor as a scalar function of the rotor position and avoids addressing the behavior of each phase for the identification of its parameters.

Methods and algorithms are then proposed for the identification of the disturbance model. They require a controlled motion where information about the torque pulsations is extracted from the output of the closed loop controller and correlated to the angular position of the rotor. Then, in order to cope with the time varying nature of the fundamental harmonic of the disturbance, online adaptation of the parameter estimates is setup.

A compensation technique is discussed as well. The idea is to modify online the current reference produced by the position controller as a function of the rotor position. As such, the algorithm can be performed directly in the position controllers, even though modifications of the lookup tables used to compute the brushless functions for the single motors would be feasible as well. Experimental results, performed on the motors of an industrial robot (COMAU SMART3S) are given to show the effectiveness of the compensation technique.

In Section 2 the sources of torque ripple are reviewed, while in Section 3 the model of the ripple is discussed. Section 4 introduces the adaptive identification of the disturbance, while Section 5 presents the compensation scheme. Experimental results are shown in Section 6.

2. TORQUE DISTURBANCE GENERATION

Consider the functional scheme of a sinusoidal PMAC machine, represented in Fig. 1.

If a reference torque $\bar{\tau}$ should be delivered by the motor, typically as required by a position controller, the current reference $\bar{I}$ has to be given the value $\bar{I} = \bar{\tau}/K_t$, where K_t is the torque constant. This scalar setpoint is then modulated through three sinusoidal functions of the electrical angle $\alpha = pq_m$, p being the number of pole pairs and q_m being the motor angle, that are offset by $2\pi/3$ one from each other. The three resulting signals become the current setpoints for the three phases. High bandwidth current controllers make the currents track their setpoints in each phase. If the current reference in each phase is given the same dependence on the electrical angle characterizing the back EMF (ideally sinusoidal or trapezoidal), a torque τ is produced, approximately equal (in a band of frequencies limited by the current loops) to the desired torque $\bar{\tau}$, and thus proportional to the scalar current reference $\bar{I}$.

The behavior of a real motor differs however from the simple one here described. Several constructive imperfections of the motor and the servodrive sum up to form a pulsating disturbance on the torque. Cogging torque and pulsating torque due to offsets in the current drives are examples of pulsating torque disturbances not related to the current reference. Cogging is mainly due to the presence of slots in the stator, where the rotor generated magnetic flux seeks a minimum reluctance path. It is present even when the drive is not connected to the power supply and depends in a periodic way on the mechanical angle. When the drive is connected to the power supply and the current reference is zero, a current offset may be present in one or both the closed loop controlled phases, and thus on the third one. These currents generate an offset torque periodic with period 2π with respect to the electrical angle α.

Pulsating torques related to the current reference are due to imperfections in the construction of the motor and the drive, implying that both the back EMF profiles and the phase currents may be affected by undesired higher order harmonics, while obviously maintaining the periodicity of 2π with respect to the electrical angle.

3. TORQUE DISTURBANCE MODEL

As it is shown in (Ferretti *et al.*, 1998*a*), the following relation can be used to represent in a compact form the effects of the disturbances on the torque production:

$$\tau = \tau(\alpha, \bar{I}) = \gamma(\alpha) + K_t\bar{I}(1 + \delta(\alpha)) \qquad (1)$$

The term $\gamma(\alpha)$ accounts for the disturbances due to the cogging torque and to the current offset in the drives, while the second term is responsible for the nominal torque (with $\delta(\alpha) = 0$) and for the disturbances related to the harmonic content. It is also possible to include in $\delta(\alpha)$ the effects of the amplitude imbalances and the phase misalignments of the current and back EMF shapes profiles (Ferretti *et al.*, 1998*a*).

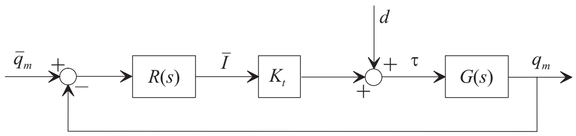

Fig. 2. Position controlled motor with torque disturbance

The functions $\gamma(\alpha)$ and $\delta(\alpha)$ in (1) are time-invariant, periodic with period 2π with respect to the electrical angle and null in nominal conditions. Notice that the formulation of the model does not require knowledge of the characteristics of the single phases (in terms of back EMF profiles, imbalances and misalignments), but only of their combined effect in the parameters of the scalar equation (1).

Fourier expansions of the functions $\gamma(\alpha)$ and $\delta(\alpha)$ are introduced in order to parametrize the model, in the following form:

$$\gamma(\alpha) = \sum_{k \in N_\gamma} \gamma_k \sin(k\alpha + \beta_k) \tag{2}$$

$$\delta(\alpha) = \sum_{k \in N_\delta} \delta_k \sin(k\alpha + \psi_k) \tag{3}$$

where N_γ and N_δ are the sets of harmonics to be considered in the expansions of $\gamma(\alpha)$ and $\delta(\alpha)$, respectively. A validation of the model, performed through several static measurements of the torque of a motor mechanically constrained in different positions and subject to different current references, has been described in detail in (Ferretti *et al.*, 1998*a*).

4. ADAPTIVE IDENTIFICATION OF THE DISTURBANCE

For the purpose of online compensation, the harmonics of the torque must be obtained from the motor through simple motion experiments. With reference to expressions (2,3), the goal of the identification is therefore to give estimates for the amplitudes γ_k and δ_k and phases β_k and ψ_k. The basic idea is to get them by examining the output of the position controller in a closed loop experiment.

Consider first the block diagram (Fig. 2) of the motor controlled by a linear regulator, where the disturbance is represented as an external input (actually, according to (1), it depends on α and $\bar{I}$), while $G(s)$ and $R(s)$ stand for the transfer functions of the process and of the regulator, respectively.

The following relation, in terms of transfer functions, is easily obtained:

$$K_t\bar{I} = \frac{K_t R(s)}{1 + L(s)}\bar{q}_m - \frac{L(s)}{1 + L(s)} d \tag{4}$$

where $L(s) = K_t R(s) G(s)$, and

$$G(s) = \frac{1}{J_m s^2 + D_m s}$$

J_m and D_m being the inertia and viscous friction coefficient of the motor respectively. Inverting (4) one obtains:

$$d = \frac{1}{G(s)}\bar{q}_m - \frac{1 + L(s)}{L(s)} K_t \bar{I} \tag{5}$$

and taking the following approximation for the closed loop transfer function of the system:

$$\frac{L(s)}{1 + L(s)} \cong \frac{1}{1 + s/\omega_c},$$

ω_c being the crossover frequency of the loop, eq. (5) can be rewritten as follows:

$$d \cong (J_m s^2 + D_m s)\bar{q}_m - (1 + s/\omega_c) K_t \bar{I}$$

finally yielding, in the time domain:

$$d \cong J_m \ddot{\bar{q}}_m + D_m \dot{\bar{q}}_m - K_t \bar{I} - \frac{K_t}{\omega_c}\dot{\bar{I}} \tag{6}$$

The reconstruction of the disturbance thus goes like this: assuming the position reference a known function of time, its first two derivatives are computed at each sampling instant, and the samples of the current reference $\bar{I}$ commanded by the position regulator are stored. The time derivative of this signal is then computed numerically, while eq. (6) gives the time series of the estimates of the disturbance.

Notice that the time derivative of the current reference required by (6) can yield noise amplification. If this is the case, this term can be neglected, provided that the spectrum of the position reference signal is entirely contained in the bandwidth of the closed loop system.

Previous studies (Ferretti *et al.*, 1998*a*) have shown that the main harmonic of the disturbance γ is associated to index $k = 1$ and is related to the current offsets in the servodrive, while the spectrum of function δ is dominated by the sixth harmonic, related to the imperfections of the nominally sinusoidal back EMF profiles. Furthermore it has been shown that the first harmonic of the current independent component $\gamma(\alpha)$ shows typically a time dependence (Ferretti *et al.*, 1998*b*), due to a thermal drift of the offset in the current sensors. In order to cope with this and other time dependences, an adaptation of the estimates is to be implemented. Here the procedure for an adaptive estimation of the principal harmonics of the disturbances $\gamma(\alpha)$ and $\delta(\alpha)$ will be shortly outlined.

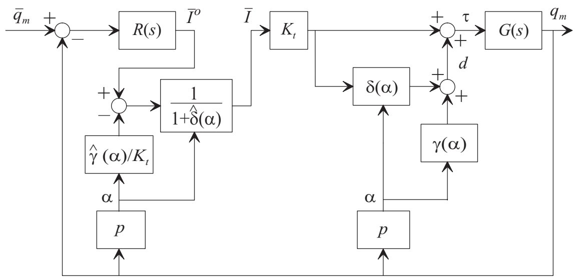

Fig. 3. Position controlled motor with compensation

The idea is simply to find the estimates for amplitudes γ_1 and δ_6 and phases β_1 and ψ_6 of the sinusoids by minimizing the following quadratic loss function:

$$J = \frac{1}{N} \sum_{i=1}^{N} \mu^{N-1} \left[d(i) - \hat{d}(i) \right]^2$$

where N is the total number of data used for the identification, $\mu \in (0, 1]$ is a suitable forgetting factor, d is evaluated as in (6) and $\hat{d}(i)$ is evaluated as follows:

$$\hat{d}(i) = \hat{\gamma}_1 \sin \left(\alpha(i) + \hat{\beta}_1 \right) + \\ + K_t \bar{I}(i) \hat{\delta}_6 \sin \left(6\alpha(i) + \hat{\psi}_6 \right)$$

Explicit formulas for the estimates of γ_1, β_1, δ_6 and ψ_6 can be obtained with this minimization. A recursive algorithm can then be setup in the form:

$$\hat{\beta}_{1,i} = \hat{\beta}_{1,i-1} + f_\beta \left(d_i, \hat{\beta}_{1,i-1}, \hat{\delta}_{6,i-1}, \hat{\psi}_{6,i-1} \right) \quad (7)$$

$$\hat{\gamma}_{1,i} = \hat{\gamma}_{1,i-1} + f_\gamma \left(d_i, \hat{\beta}_{1,i-1}, \hat{\gamma}_{1,i-1}, \hat{\delta}_{6,i-1}, \hat{\psi}_{6,i-1} \right) \quad (8)$$

$$\hat{\psi}_{6,i} = \hat{\psi}_{6,i-1} + f_\psi \left(d_i, \hat{\beta}_{1,i-1}, \hat{\gamma}_{1,i-1}, \hat{\psi}_{6,i-1} \right) \quad (9)$$

$$\hat{\delta}_{6,i} = \hat{\delta}_{6,i-1} + f_\delta \left(d_i, \hat{\beta}_{1,i-1}, \hat{\gamma}_{1,i-1}, \hat{\delta}_{6,i-1}, \hat{\psi}_{6,i-1} \right) \quad (10)$$

where second subscript i denotes step i. Details on functions f_β, f_γ, f_ψ and f_δ can be found in (Sommaruga, 1999).

5. DESIGN OF A COMPENSATION TECHNIQUE

Once the estimates for functions $\gamma(\alpha)$ and $\delta(\alpha)$ have been obtained, from the recursive least squares algorithm sketched in Section 4, a compensation scheme as in Fig. 3 can be setup. Let $\bar{I}^o$ be the current reference determined on the basis of a model of the motor free of the disturbances. In other words, let $\bar{I}^o = \bar{\tau}/K_t$, where $\bar{\tau}$ is the torque that the motor is supposed to deliver. The actual current reference will be determined as follows:

Fig. 4. Robot COMAU SMART3S

$$\bar{I} = \frac{\bar{I}^o - \hat{\gamma}(\alpha)/K_t}{1 + \hat{\delta}(\alpha)}$$

This way, if the estimates are ideally exact ($\delta(\alpha) = \hat{\delta}(\alpha)$, $\gamma(\alpha) = \hat{\gamma}(\alpha)$), the effect of the disturbance is completely eliminated.

Thus the estimates $\hat{\gamma}(\alpha)$ and $\hat{\delta}(\alpha)$ are used to continuously (i.e. at every sampling instant) modify the current reference $\bar{I}^o$ produced by a closed loop controller.

6. EXPERIMENTAL RESULTS

The experiments have been made on the industrial robot SMART3S (Fig. 4), manufactured by COMAU, endowed with an open version of its controller C3G 9000. The robot SMART 3S is a 6 d.o.f., 6 Kg payload manipulator. PMAC brushless motors are used in all the joints: specifically the first three joints (positioning joints) mount SIEMENS 1FT75048-OAH21 motors (nominal torque 2.7 Nm) while the last three joints (wrist joints) mount SIEMENS 1FT5036-OAH01 motors (nominal torque 0.8 Nm). The controller C3G 9000 is based on a Motorola VME bus with two single board computers mounting Motorola CPUs. In the open version, it is interfaced to a PC by means of a bus-to-bus connection made up by two boards manufactured by BIT3. Every ms the PC receives an interrupt from the C3G, and, for each joint, reads the motor position in a memory shared with the Motorola CPUs, computes a new current reference (on the basis of a precomputed position set-point and of a suitable PID control

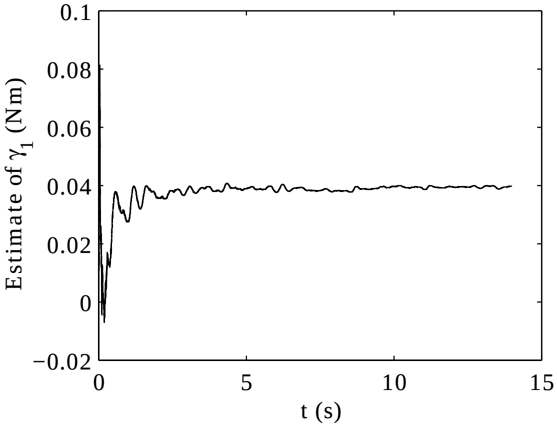

Fig. 5. Time history of the estimate of γ_1

law) and writes the current reference into the shared memory. Both the motor positions and the current references are stored every ms.

A first experiment has been run on the first link, commanding a 5 rad/s constant velocity motion. The recursive algorithm (7–10) has been used to implement an adaptive compensation of the first harmonic of the two disturbances. In the first part of the experiment, the compensation is kept off and the recursive algorithm works to update the estimates of the amplitudes and phases of the disturbances. When these estimates reach a steady value, the compensation is switched on, while the recursive algorithm keeps updating the estimates. In this experiment the compensation has been switched on after 5 seconds. The evolution of the estimates for the amplitudes of the harmonics is shown in Fig. 5 and Fig. 6 (the estimates of the phases follow a similar evolution). Fig. 7 reports the motor velocity, as numerically computed from the position measurements. The role of the compensation in suppressing the disturbance harmonic is quite evident.

The motor velocity, derived from the position measurements, has been Fourier analyzed with respect to time before and after compensation, for validation purposes. The amplitudes of the harmonics are compared in Fig. 8, where it is apparent that the harmonic at 15 rad/s (corresponding to $k = 1$, as the motor has 3 pole pairs) and the harmonic at 90 rad/s (corresponding to $k = 6$) have been reduced to about 3% and 16%, respectively, of their values without compensation. The other harmonics are left almost unchanged.

Finally, a force sensor has been mounted on the end effector, in order to achieve an indirect measure of the acceleration of the tip of the robot: this is useful to investigate the behavior of the load, which cannot be simply inferred from the behavior of the motor, due to the decoupling effect played by the elastic transmission. The force measured in the tangential direction in an experiment with

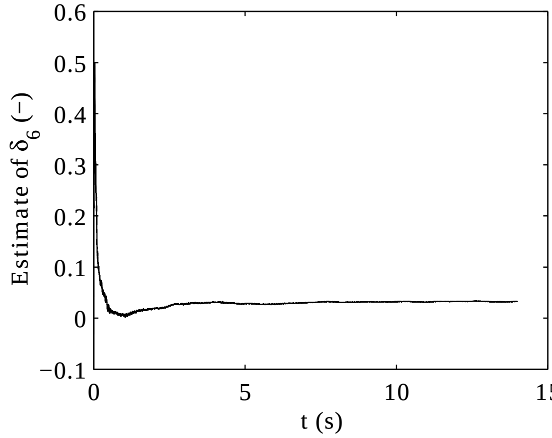

Fig. 6. Time history of the estimate of δ_6

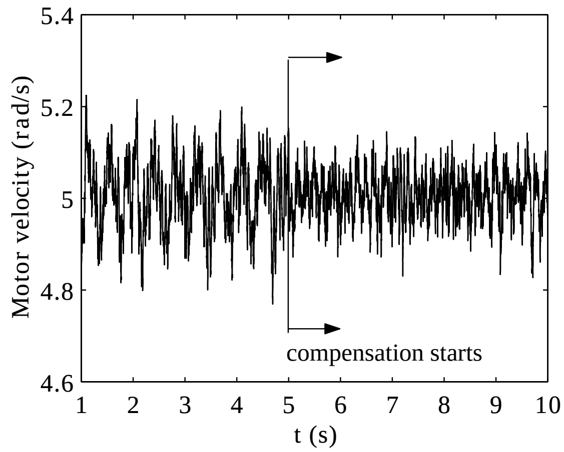

Fig. 7. Time history of the velocity

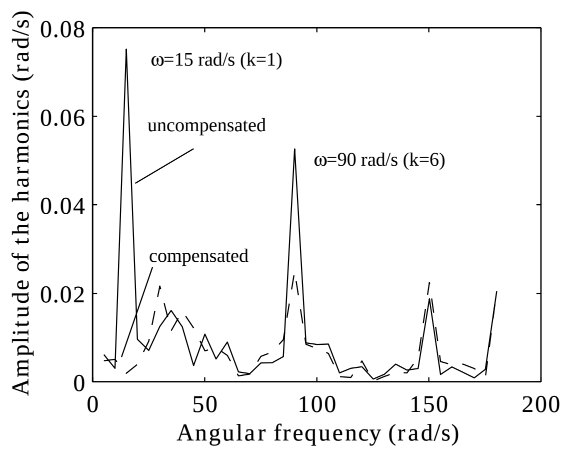

Fig. 8. Amplitudes of the harmonics of the motor velocity

coordinated motion of the first three joints has been recorded, divided by the payload mass (2 Kg), integrated (to get the linear velocity of the end effector) and Fourier analyzed. The comparison (Fig. 9) of the amplitudes of the harmonics obtained replies the same results of Fig. 8, which proves the efficacy of the control scheme in the suppression of the load oscillations. Notice that a new harmonic with frequency equal to 50 rad/s

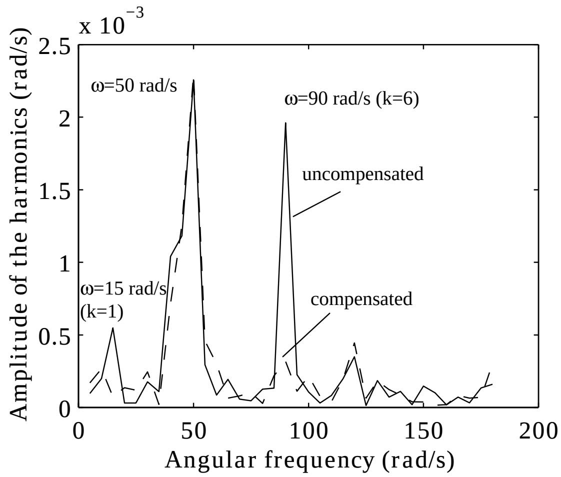

Fig. 9. Amplitudes of the harmonics of the end effector velocity

(ten times the average angular velocity of the motor) appears, identically with and without compensation. It has been ascribed to resolver noise (Hanselman, 1991) and cannot be compensated for with the methodology described in the present paper.

7. CONCLUSIONS

The reduction of the torque pulsation at source level is the most promising approach to the suppression of load oscillation at low velocity, in servomechanisms and in robotics. Therefore a compact model of pulsating torque disturbances suitable for online compensation has been given, together with algorithms for adaptive identification of the motor parameters. Experiments have been given which show the effectiveness of this approach for disturbance compensation.

8. REFERENCES

Clenet, S., Y. Lefèvre, N. Sadowski, S. Astier and M. Lajoie-Mazenc (1993). Compensation of permanent magnet torque ripple by means of current supply waveshapes control determined by finite element method. *IEEE Transactions on Magnetics* **29**, 2019–2023.

Favre, E., L. Cardoletti and M. Jufer (1993). Permanent-magnet synchronous motors: a comprehensive approach to cogging torque suppression. *IEEE Transactions on Industrial Applications* **29**, 1141–1149.

Ferretti, G., G. Magnani and P. Rocco (1998*a*). Modelling, identification and compensation of pulsating torque in permanent magnet ac motors. *IEEE Transactions on Industrial Electronics* **46**(6), 912–920.

Ferretti, G., G. Magnani and P. Rocco (1998*b*). Online identification and compensation of torque disturbances in permanent magnet ac motors. In: *Proc. 2001 IECON'98*. Aachen, Germany. pp. 1521–1526.

Hanselman, D. (1991). Techniques for improving resolver-to-digital conversion accuracy. *IEEE Transactions on Industrial Electronics* **38**(6), 501–504.

Hanselman, D. (1994). Minimum torque ripple, maximum efficiency excitation of brushless permanent magnet motors. *IEEE Transactions on Industrial Electronics* **41**, 292–300.

Holtz, J. and L. Springob (1996). Identification and compensation of torque ripple in high-precision permanent magnet motor drives. *IEEE Transactions on Industrial Electronics* **43**(2), 309–320.

Hung, J. Y. and Z. Ding (1993). Design of currents to reduce torque ripple in brushless permanent magnet motors. *IEE Proceedings - Part B* **140**, 260–266.

Jahns, T. M. (1984). Torque production in permanent-magnet synchronous motor drives with rectangular current excitation. *IEEE Transactions on Industrial Application* **20**, 803–813.

Jahns, T. M. and W. L. Soong (1996). Pulsating torque minimization techniques for permanent magnet ac motor drives - a review. *IEEE Transactions on Industrial Electronics* **43**(2), 321–330.

Le-Huy, H., R. Perret and R. Feuillet (1986). Minimization of torque ripple in brushless dc motor drives. *IEEE Transactions on Industrial Applications* **22**, 748–755.

Sommaruga, S. (1999). Adaptive compensation of torque disturbances in the brushless motors of an industrial robot (in italian). Master's thesis. Politecnico di Milano.